Density Functional Theory Study on the Electronic Structure and Optical Properties of La, Ce and Nd doped SnO_2

Shao Tingting Zhang Fuchun Cui Hongwei

College of Physics and Electronic Information, Yan'an University, Yan'an, Shaanxi 716000, China

Abstract The lattice parameters, band structures, density of states, electron density differences and optical properties of La, Ce, Nd doped SnO_2 are studied by density functional theory (DFT). The computational results show that the bond length near La are greatest changed, while the change near Nd are least, which indicates the lattice distortion caused by rare earth doped in SnO_2 is related to the covalent radius of doping atom. The band structure shows that rare earth doping can make the band gap of SnO_2 narrow. The La doping makes the band gap reduced 0.892 eV comparing that of intrinsic SnO_2, and Nd doping induces three energy levels in the forbidden band. The electron density difference shows that rare earth doping makes the electron redistribution of SnO_2 and the iconicity enhance, especially the existence of f electrons. La atom loses electrons most and Nd atom loses least, which are consistent with the calculated results of band gaps. The calculated results of optical properties show that the imaginary part of the dielectric function and absorption function have a red shift, which agrees well with the calculated results of energy band gap.

Key words materials; SnO_2; rare earth doping; density functional theotry; electronic and optical property

OCIS codes 160.4236; 160.5690; 160.6000

La, Ce, Nd掺杂SnO_2的电子结构和光学性质密度泛函理论研究

邵婷婷 张富春 崔红卫

延安大学物理与电子信息学院, 陕西 延安 716000

摘要 基于平面波赝势密度泛函理论,研究了La, Ce, Nd掺杂SnO_2的电子结构和光学性质。计算结果表明,La附近的键长变化最大,而Nd附近的键长变化最小,这表明稀土掺杂SnO_2引起的晶格畸变与掺杂原子的共价半径大小有关。能带结构表明,稀土掺杂可使SnO_2的带隙变窄。La掺杂相比较本征SnO_2,带隙减小了0.892 eV, Nd掺杂在SnO_2的禁带中引入了3个能级。差分电荷密度分析表明,稀土掺杂使SnO_2的电子重新分配且由于f电子的存在使其离子性增强。La原子失电子最多,Nd原子失电子最少,这和计算的能带结果是一致的。光学性质表明,介电函数的虚部和吸收函数因稀土掺杂出现了不同程度的红移,这和计算的能带结果非常吻合。

关键词 材料; SnO_2; 稀土掺杂; 密度泛函理论; 电学和光学性质

中图分类号 O471.4 **文献标识码** A

doi: 10.3788/LOP52.091602

1 Introduction

Stannic oxide (SnO_2), whose experimental band gap is 3.6 eV, has high exciton binding energy (130 meV in experiment)[1]. SnO_2 is an n-type wide band-gap semiconductor, because there is oxygen vacancy in its crystal lattice and form a -0.15 eV donor level. SnO_2 has attracted increasing interests and has potential

收稿日期: 2015-01-27; **收到修改稿日期**: 2015-03-31; 网络出版日期: 2015-08-20

基金项目: 陕西省自然科学基础研究计划(2014JM2-5058)、陕西省教育厅科学研究计划(2013JK0917)、延安市科学技术研究发展计划(2013KG-03,2014KG-02)

作者简介: 邵婷婷(1982—),女,硕士研究生,讲师,主要从事纳米材料光电性质方面的研究。E-mail: retastt@126.com

导师简介: 张富春(1972—),男,博士,副教授,主要从事纳米光电子材料方面的研究。

E-mail: zhangfuchun72@163.com(通信联系人)

applications such as catalytic support material, transparent electrodes for liquid crystal displays (LCDs), solar cells, chemical gas sensors, and optoelectronic devices[2-3]. Doping is one of the most important processes in semiconductor and integrated circuits fabrication, and the photoelectric characteristics can be controlled by selection of impurities and adjusting of impurities concentration[4]. The new materials formed by doped SnO_2 have higher conductivity and better optical transmittance, and the research on metallic ion doped SnO_2 compound has involved some theoretical and experimental investigations. Du et al.[5] studied the electronic properties of Ⅲ family doped SnO_2, which pointed out that In-doped SnO_2 could achieve best p-type result at the same doping concentration. Yu et al.[6-7] calculated the density of states and optical properties of Al, N doped SnO_2, which showed that the corresponding spectral line made a blue shift. Lu et al.[8] studied the electronic structure and optical properties of Fe-doped SnO_2, which discovered that the doped SnO_2 had half-metallic property.

Rare earth atom doping is widely investigated in the wide band gap semiconductor system, as the rare earth atoms have un-filled 4f and 5d electron configuration, rich electronic energy levels and long period excited states[9-10]. There are some preparation reports about rare earth elements doping SnO_2 based electrodes. Bi et al.[11] studied the effect of lanthanum doping Ti/Sb-SnO_2 electrode, which pointed out that the electrode doped with La is superior for the treatment of p-NP wastewater. Liu et al.[12] studied the effect of SnO_2 electrothermal film doped with Ce. Li et al.[13] prepared the electro-catalytic electrodes of neodymium doped Ti-based SnO_2/Sb and found that the average size of SnO_2 grains on the electrode surface of Nd doped SnO_2 electrode was smaller. Zhu et al.[14] studied the effect of properties of europium doped Ti/SnO_2-Sb electrode and found that Eu doping can make the elecrode had higher oxygen evolution potential. However, the first principle simulative calculation of electronic structure and properties of rare earth atoms doped SnO_2 are still not reported so far.

In this paper, the structural, electronic and optical properties of La, Ce and Nd doped SnO_2 based on density functional theory (DFT) with generalized gradient approximation (GGA) are calculated. The calculations contain lattice constant, band structure, density of state, electron density difference, dielectric and absorption function, which are expected to study the effect of crystal structure, electronic properties and optical properties about rare earth doping of SnO_2.

2 Method for calculation and theoretical descriptions

2.1 Method for calculation

Theoretical calculations are performed by plane wave pseudo potential method based on the DFT[15]. Using pseudo-potentials to replace ionic potentials, the electronic wave function is expanded by plane wave basis sets. The related potential and electron-electron exchange are rectified by the GGA, which is an accurate theory method of electronic structure calculation[16-17]. The properties of intrinsic, and La, Ce, and Nd doped SnO_2 system are calculated through the vienna Ab-initio simulation package (VASP) program[18]. As shown in Fig.1, the SnO_2 2×2×2 super cell contains 16 Sn atoms and 32 O atoms, and one rare earth atom is used to replace one Sn atom showing as X, whose doping concentration are all 6.25%. References[11-13] show that the concentration ratio of X/Sn can achieve 6.25% in technological process, and when the concentration ratio of Ce/Sn is 6%, the thermal stability of electrical properties is good. In the calculation, the lattice constants are based on the experimental results (a=b=0.4737 nm, c=0.3186 nm, $\alpha=\beta=\gamma=90°$ [19]). The energy cut-off of plane wave takes 340 eV, while Monkhorst - Pack mesh of Brillouin-Zone sampling takes 5×5×8, and the self-consistent convergence of the total energy takes 1×10^{-6} eV/atom for both super cells. The parameters after optimized are all achieve convergence criteria. The atomic configuration for O, Sn, La, Ce and Nd are $2s^2 2p^4$, $5s^2 5p^2$, $5p^6 5d^1$, $5p^6 5d^1 4f^1$ and $5p^6 5d^0 4f^4$ respectively. For intrinsic SnO_2, the net charge between Sn atom and Sn atom is all 0.58 e, and the net charge between O atom and Sn atom is all -0.29 e, which means that

same atoms are equivalent.

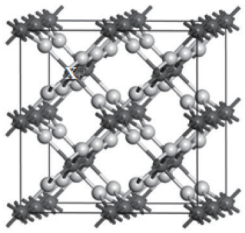

Fig.1 SnO_2 2×2×2 super cell (black ball is Sn atom, grey ball is O atom, the Sn of position X is substituted for La, Ce and Nd, respectively)

2.2 Theoretical descriptions

In linear response range, the complex dielectric function $\varepsilon(\omega)=\varepsilon_1(\omega)+i\varepsilon_2(\omega)$ is used to describe the solid macro-optical response. Where $\varepsilon_1=n^2-k^2$, $\varepsilon_2=2nk$ and n is the reflection coefficient, k stands for the extinction coefficient[20]. The real part can be obtained by Kramer-Kroing dispersion relation and imaginary part can be obtained by momentum matrix elements of wave function between occupied states and unoccupied states[21-22]. The derivation process is ignored, and only giving the results.

$$\varepsilon_1(\omega)=1+\frac{8\pi^2e^2}{m^2}\sum_{V,C}\int_{B_Z}d^3k\frac{2}{2\pi}\frac{\left|eM_{CV}(K)\right|^2}{\left[E_C(K)-E_V(K)\right]}\times\frac{h^3}{\left[E_C(K)-E_V(K)\right]^2-h^2\omega^2}, \tag{1}$$

$$\varepsilon_2(\omega)=\frac{4\pi^2}{m^2\omega^2}\sum_{V,C}\int_{B_Z}d^3k\frac{2}{2\pi}\left|eM_{CV}(K)\right|^2\times\delta\left[E_C(K)-E_V(K)-h\omega\right], \tag{2}$$

$$I(\omega)=\sqrt{2}(\omega)\left[\sqrt{\varepsilon_1(\omega)^2-\varepsilon_2(\omega)^2}-\varepsilon_1(\omega)\right]^{\frac{1}{2}}, \tag{3}$$

$$R(\omega)=\frac{(n-1)^2+k^2}{(n+1)^2+k^2}, \tag{4}$$

Where C, V represents conduction band and valence band, B_Z is first Brillouin-zone, K is reciprocal vector, $\left|eM_{CV}(K)\right|^2$ is transition matrix element, and ω is angular frequency. The above equations are the theory evidences of analyzing crystal band structure and optical properties. They reflect the Luminescence mechanism generated by the electronic transitions between the energy levels.

3 Results and discussion

3.1 Lattice distortion around La, Ce and Nd impurity

The calculated results after geometry optimization of intrinsic and rare earth doped SnO_2 super cells are shown in Table 1. Where d_{X-Sn} is the bond length between X atom and its nearest Sn atom, d_{X-O} is the bond length between X atom and its nearest O atom, d_{O-O} is the bond length of two O atoms which are nearest to X atom, r_X is the covalent radius of X atom, and θ_{O-X-O} is the bond angle of X atom and two O atoms which are at the same plane.

Table 1 Structure parameters of intrinsic and rare earth doped SnO_2 after geometry optimization, X=Sn, La, Ce, Nd

Doping atom	d_{X-Sn} /nm	d_{X-O} /nm	d_{O-O} /nm	r_X /nm	θ_{O-X-O} /(°)
Intrinsic SnO_2	0.3156	0.2034	0.2567	0.141	78.271
La	0.3315	0.2341	0.2880	0.169	75.942
Ce	0.3296	0.2265	0.2807	0.165	76.555
Nd	0.3218	0.2259	0.2838	0.164	77.829

As shown in Table 1, comparing with the crystal lattice parameters of intrinsic SnO_2, rare earth doping induces lattice distortion around impurity atom, but the distortions are different. The bond length changes around La are the biggest, and those nearby Ce take the second place, while those adjacent Nd are almost the least. When a La atom replaces a Sn atom, the variations of bond length d_{La-Sn} and d_{La-O} are

5.04% and 15.09%, respectively, and the variations of bond length d_{O-O} and bond angle θ_{O-La-O} are 12.19% and 2.98% respectively. When a Nd atom replaces a Sn atom, the variations of bond length d_{Nd-Sn} and d_{Nd-O} are 1.96% and 11.06%, respectively, and the variations of bond length d_{O-O} and bond angle θ_{O-Nd-O} are 10.56% and 0.56%, respectively, which are far less than the results of La and Ce doping. The difference of super cells lattice distortion is mainly due to the covalent radius difference of doping atoms. The covalent radius differences of Sn and Ce, Nd are 0.024 nm, 0.023 nm, respectively, which are all less than that of Sn and La, 0.028 nm.

3.2 Band structure and density of state

The energy band structures of intrinsic and rare earth doped SnO_2 are shown in Fig.2. The Fermi level is chosen to be zero of the energy scale, and energy range takes −6~6 eV.

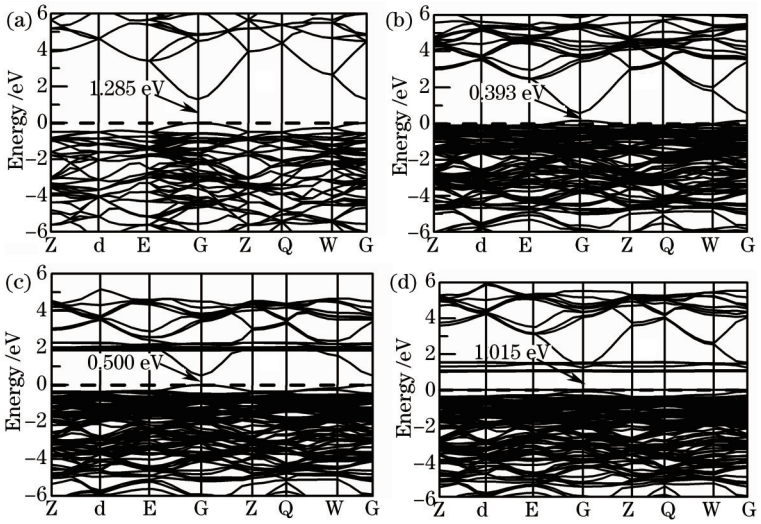

Fig.2 Band structure graph of SnO_2. (a) Intrinsic; (b) La doping; (c) Ce doping; (d) Nd doping

As shown in Fig.2, the rare earth doped SnO_2 are direct band-gap semiconductor like intrinsic SnO_2, whose energy band gap is 1.285 eV and there is no energy level in the forbidden band. The band gaps are 0.393, 0.500 and 1.015 eV for La, Ce and Nd doped SnO_2, respectively. The calculated band gaps are all lower than available experimental data (3.7~3.8 eV) mentioned in paper[23], and this is because GGA is ground state theory, and the energy-gap belongs to property of excited state[24]. La, Ce doping make the band gap reduced much more, while Nd doping makes that reduced less, because there are *d* state electrons in La and Ce atoms while there is no *d* state electron in Nd. The energy states are mainly focus on the low energy region of conduction band for rare earth doped SnO_2, and there are more energy levels in both conduction band and valence band than intrinsic SnO_2, which is consistent with the rich energy levels of rare earth impurity. In addition, Nd doping induces three energy levels in the forbidden band around 1 eV, which are possibly donor levels, but it may also have one acceptor level.

The total density of state (TDOS), partial density of states (PDOS) of intrinsic SnO_2 and rare earth doped SnO_2 are shown in Fig.3. According to the energy concentrated region and convenient analysis, −23~8 eV is choosed as the energy region for intrinsic and rare earth doped SnO_2. From the Fig.3, it can be seen that the conduction band of intrinsic SnO_2 is wider than that of rare earth doped SnO_2, which is the narrowest in Ce doping, and it is just ended at 5 eV. The energy state in high energy region disappears, because there are some *s* orbital electrons restriction that caused by the hybridizations between rare earth atoms and their nearest O atoms. For the intrinsic SnO_2, the conduction band is mainly dominated by Sn $5p^2$ and Sn $5s^2$, and O $2p^4$ have a few contributions. However, there are also contributions from 5d and 4f electrons of impurity atoms for rare earth doped SnO_2, especially for Ce and Nd doped SnO_2. The 4f electrons of impurity atoms contribute obviously. The main peak position of density of state for Nd $4f^4$ is in the forbidden band, which

fits the band structure analysis above. Valence band can be divided into two parts, the low valence band, −23~−10 eV regions, which is dominated by O $2s^2$ states, with a minor-presence of Sn $5s^2$ and Sn $5p^2$ states for intrinsic SnO_2. In addition, there are also some contributions from 5p electrons of impurity atoms for rare earth doped SnO_2. The low valence band can be ignored because it is far from Fermi level that has little influence with it. The high valence band, −10~0 eV region is dominated by Sn $5s^2$, Sn $5p^2$ and O $2p^4$ states, especially closed to Fermi level, O $2p^4$ state is dominated, and with a few contributions of 5d and 4f states of rare earth atoms for rare earth doped SnO_2, it illustrates that O atom can absorb electrons strongly from rare earth atoms and Sn atom. It is noticed that Nd has no d state electron in electron configuration, but there are d state electrons in Nd-doped SnO_2 super cell. This is because in the hybrid bonding of Nd atom and O atom, Nd 6s electrons transit to 5d electrons and then hybrid with O 2p state electrons, which may reduce the total energy.

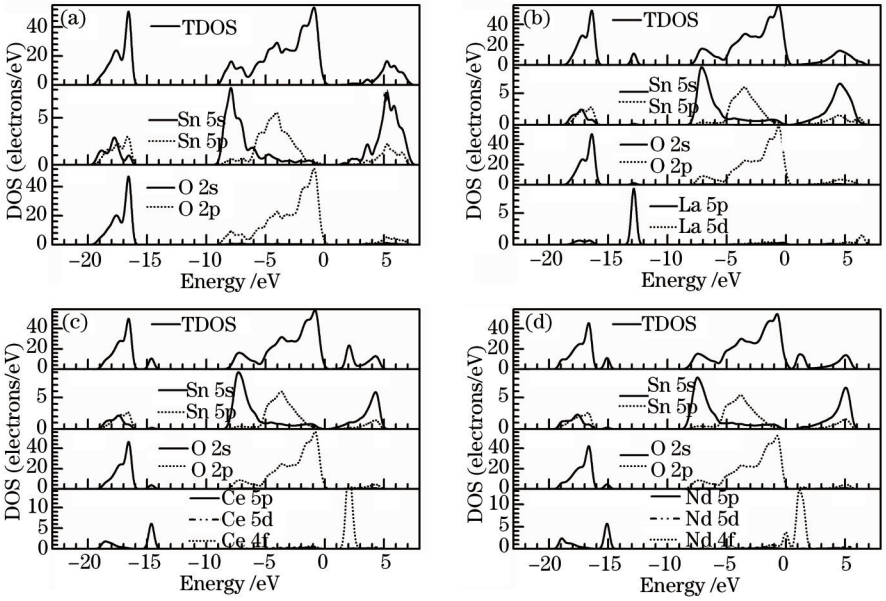

Fig.3 TDOS and PDOS graph of SnO_2. (a) intrinsic; (b) La doping; (c) Ce doping; (d) Nd doping

3.3 Charge density difference

In order to study the electron distribution effects of rare earth doping for SnO_2 and show the image of redistributed charge caused by rare earth impurity, the charge density difference in the (1 1 1) basal plane of intrinsic SnO_2 and rare earth doped SnO_2 are calculated and the graphs are shown in Fig.4.

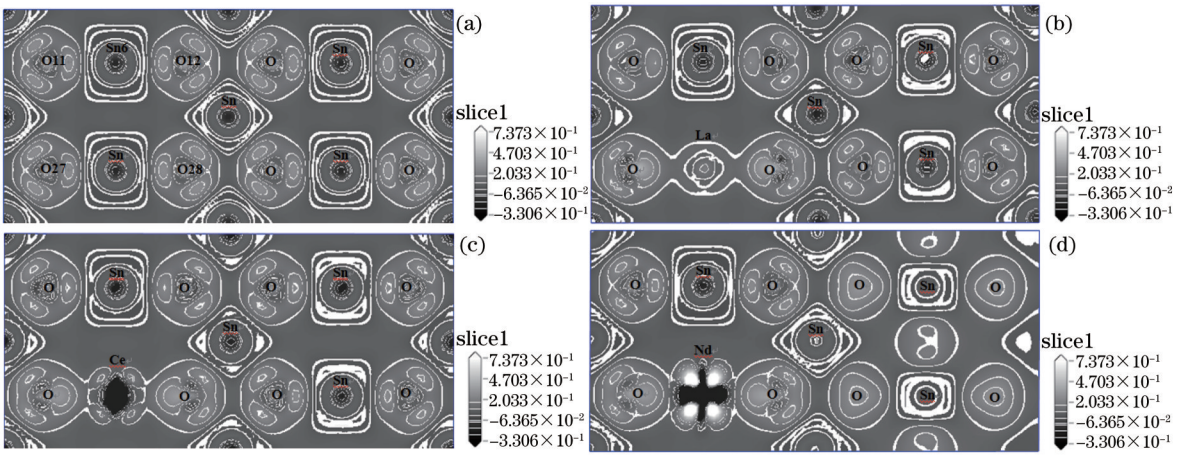

Fig.4 Charge density difference graph of SnO_2. (a) Intrinsic; (b) La doping; (c) Ce doping; (d) Nd doping

As shown in Fig.4, the same gray scale is given on the right, and the charge density difference values of black region are negative, which represent electron losing. In contrast, the charge density difference values

of white region are positive, which represent electron gathering. Figure 4 shows that the charge density difference is very different between intrinsic SnO_2 and rare earth doped SnO_2, and the charge is redistributed. For intrinsic SnO_2, the charge density difference around Sn atoms or around O atoms are the same respectively, but they are different between each other. The regions around Sn atoms, especially in the bonding direction of Sn-O, are mainly black, which means electrons losing, while those around O atoms are contrast. The Fig.4 (a) is formed, because Sn atoms loss electrons easily and O atoms obtain electrons easily. La, Ce and Nd doped SnO_2 show different results. For the charge density difference around rare earth atoms, the regions about La are mainly gray, whose gray levels are lower than Sn atoms, which represent La atom losses less electrons than Sn atom. Ce, Nd doping are different from La doping, and the regions around Ce, Nd are all black but the distributions of charge density difference are not same, especially the region around Nd has a clear distinction between black and white, that is, there are not only electrons losing but also electrons gathering, which is consistent with the analysis of band structure above. The great contrast charge density difference graph is possibly related to the 4f orbital electrons.

In order to understand the change of electron transfer and bonding, some of the atomic and bond populations around Sn and rare earth atoms are listed in the Table 2 and Table 3. Where E_X is the gain electron number of X atom, E_{Sn6} is the gain electron number of Sn atom that is nearest to X atom, E_{O11} and E_{O12} are the gain electron numbers of two O atoms which are nearest to Sn_6 atom, E_{O27} and E_{O28} are the gain electron numbers of two O atoms which are nearest to X atom, and P are the bond populations between two atoms. The positions of Sn_6, O_{11}, O_{12}, O_{27} and O_{28} are shown in Fig.4 (a).

Table 2 Atomic populations of intrinsic and rare earth doped SnO_2 X=Sn, La, Ce, Nd

Doping atom	E_X /(e)	E_{Sn6} /(e)	E_{O11} /(e)	E_{O12} /(e)	E_{O27} /(e)	E_{O28} /(e)
Intrinsic SnO_2	−1.85	−1.85	0.93	0.93	0.93	0.93
La	−1.72	−1.73	0.90	0.90	0.90	0.90
Ce	−1.37	−1.82	0.92	0.92	0.92	0.92
Nd	−1.13	−1.84	0.94	0.94	0.94	0.94

Table 3 Bond populations of intrinsic and rare earth doped SnO_2 X=Sn, La, Ce, Nd

Doping atom	P_{O27-X}	P_{O28-X}	$P_{O11-Sn6}$	$P_{O12-Sn6}$
Intrinsic SnO_2	0.39	0.39	0.39	0.39
La	0.26	0.26	0.30	0.30
Ce	0.35	0.35	0.34	0.34
Nd	0.38	0.38	0.36	0.36

As shown in Table 2, the electron transfer of intrinsic SnO_2 is different with rare earth doped SnO_2. Rare earth doping makes atom Sn_6 losing less electrons and rare earth atoms also loss electrons but less than substituted Sn atom, which are consistent with the analysis of charge density difference above. The O atoms are all gain similar electrons, which means electrons gather from rare earth atoms to O atoms. From Table 3, it is found that that the bond populations of intrinsic SnO_2 are all 0.39, and those of rare earth doping SnO_2 all diminish, especially La doping decreases the most and Nd doping decreases the least, which means that rare earth doping can make the iconicity enhance and La doping increases maximum. The analysis is consistent with the calculated result of band structures above.

3.4 Optical property

The imaginary part of complex dielectric function $\varepsilon_2(\omega)$ of intrinsic SnO_2 and rare earth doped SnO_2 from the polarization vectors [1 1 0] are shown in Fig.5. Figure 5 shows that the points of curves beginning to rise are very consistent with the calculated energy gaps, and the rise curve position of La doping is approximately at 1, which may because La doping makes Fermi level coming into valence band. The spectral lines of intrinsic and La doped SnO_2 are similar but very different with those of Ce

and Nd doping SnO_2. For Ce and Nd doped SnO_2, there are two clear peaks at the low energy region. The position of first peak is at about 2.5 eV, which arises from O $2p^4$ orbits to rare earth atom 4f ^{4} orbits, and the second peak is at about 5.2~6.5 eV, which mainly results from O $2p^4$ orbits to Sn $5s^2$ orbits, and some arise from Sn $5p^2$ orbits to the bottom of conduction band. For La doped SnO_2, the peaks of position 2 and 3 are correspond with the peaks of position 1 and 2 of Ce, Nd doped SnO_2, and the first peak appears because of the electronic transition from top of valence band to bottom of conduction band.

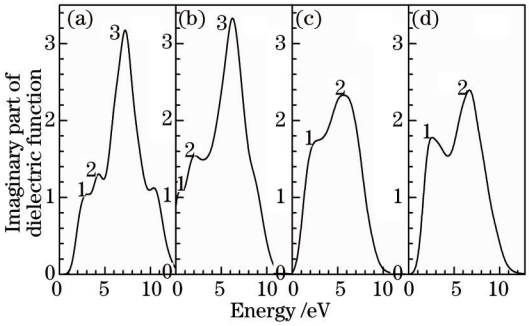

Fig.5 Imaginary part of complex dielectric graph of SnO_2. (a) Intrinsic; (b) La doping; (c) Ce doping; (d) Nd doping

The absorption function of intrinsic SnO_2 and rare earth doped SnO_2 from the polarization vectors [1 1 0] are shown in Fig.6.

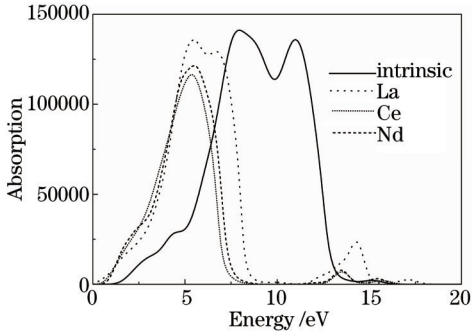

Fig.6 Absorption function graph of intrinsic SnO_2 and rare earth doped SnO_2

As shown in Fig.6, the absorption lines of rare earth doped SnO_2 have a red shift to low energy direction compared with intrinsic SnO_2. La doping has a maximum red shift and Nd doping has a minimum red shift, which agrees well with the calculated results of energy band gap.

4 Conclusion

In conclusion, the electronic structures and optical properties of both intrinsic and La, Ce, Nd doped SnO_2 by DFT are studied. The rare earth doping induces the lattice distortion as the different covalent radii of doping atoms. The band gap of SnO_2 becomes narrow after doping. Rare earth doping also changes the electron distribution and makes the iconicity enhanced. The calculated dielectric peaks are analyzed, which shows the relationship with the electronic transition from valence band to conduction band, and rare earth doping can cause absorption function having different degrees of red shift, which is consistent with the calculated results of energy band gap.

References

1 Batzill M, Katsiev K, James M, *et al*.. Gas-phase-dependent properties of SnO_2 (110), (100), and (101) single-crystal surfaces: Structure, composition, and electronic properties[J]. Phys Rev B, 2005, 72(1): 165414-20.

2 Bataill M, Diebold U. The surface and materials science of tin oxide[J]. Prog Surf Sci, 2005, 79(2-4): 47-154.

3 Liu C M, Chen X R, Ji G F. First-principles investigations on structural, elastic and electronic properties of SnO_2 under pressure[J]. Comp Mater Sci, 2011, 50(4): 1571-1577.

4 Lei Tianmin, Wu Shengbao, Zhang Yuming, *et al*.. Effect of La, Ce and Nd doping on the electronic structure of monolayer MoS_2[J]. Acta Phys Sin, 2014, 63(6): 067301.
雷天民, 吴胜宝, 张玉明, 等. La, Ce, Nd掺杂对单层MoS_2电子结构的影响[J]. 物理学报, 2014, 63(6): 067301.
5 Du Juan, Ji Zhenguo. The effect of Ⅲ-family element doping on electronic structures and electrical characteristics of SnO_2[J]. Acta Phys Sin, 2007, 56(4): 2388-2392.
杜 鹃, 季振国. Ⅲ族元素掺杂对SnO_2电子结构及电学性能的影响[J]. 物理学报, 2007, 56(4): 2388-2392.
6 Yu Feng, Wang Peiji, Zhang Changwen. Electronic structure and optical properties of Al-doped SnO_2[J]. Acta Phys Sin, 2011, 60(2): 023101.
于 峰, 王培吉, 张昌文. Al掺杂SnO_2材料电子结构和光学性质[J]. 物理学报, 2011, 60(2): 023101.
7 Yu Feng, Wang Peiji, Zhang Changwen. First-principles study of optical and electronic properties of N-doped SnO_2[J]. Acta Phys Sin, 2010, 59(10): 7285-7290.
于 峰, 王培吉, 张昌文. N掺杂SnO_2材料光电性质的第一性原理研究[J]. 物理学报, 2010, 59(10): 7285-7290.
8 Lu Yao, Wang Peiji, Zhang Changwen, *et al*.. First-principles calculation on electronic structure and optical properties of iron-doped SnO_2[J]. Acta Phys Sin, 2011, 60(11): 113101.
逯 瑶, 王培吉, 张昌文, 等. 第一性原理研究Fe掺杂SnO_2材料的光电性质[J]. 物理学报, 2011, 60(11): 113101.
9 Dar A, Majid A. Electronic structure analysis of rare earth ions Ce and Nd doped gallium nitride[J]. J Appl Phys, 2013, 114 (12): 123703.
10 Li Honglin, Zhang Zhong, Lü Yingbo, *et al*.. First principle study on the electronic and optical properties of ZnO doped with rare earth[J]. Acta Phys Sin, 2013, 62(4): 047101.
李泓霖, 张 仲, 吕英波, 等. 第一性原理研究稀土掺杂ZnO结构的光电性质[J]. 物理学报, 2013, 62(4): 047101.
11 Bi Qiang, Xue Juanqin, Yu Lihua, *et al*.. Influences of lanthanum doping on characteristics of Ti/Sb-SnO_2 electrode[J]. Journal of the Chinese Society of Rare Earths, 2013, 31(4): 465.
毕 强, 薛娟琴, 于丽花, 等. 镧掺杂对Ti/Sb-SnO_2阳极电催化性能影响的研究[J]. 中国稀土学报, 2013, 31(4): 465.
12 Liu Wensheng, Huang Wende, Yun Yuehou, *et al*.. Effect of doping CeO_2 on properties of SnO_2 electro-thermal film[J]. Journal of the Chinese Society of Rare Earths, 2005, 23(S): 74-76.
刘文生, 黄文德, 云月厚, 等. 掺杂CeO_2对制备SnO_2电热膜电学性能的影响[J]. 中国稀土学报, 2005, 23(S): 74-76.
13 Li Shanpin, Hu Zhen, Cao Hanlin, *et al*.. Preparation and characterization of neodymium doped Ti- based SnO_2/Sb electro-catalytic electrodes[J]. Journal of the Chinese Society of Rare Earths, 2008, 26(3): 291-296.
李善评, 胡 振, 曹翰林. 等. 钕改性钛基SnO_2/Sb电催化电极的制备及表征[J]. 中国稀土学报, 2008, 26(3): 291-296.
14 Zhu Fuliang, Huang Xiuyang, Yu Xibo, *et al*.. Effects of calcining temperature on properties of europium doped Ti/SnO_2-Sb electrode[J]. Journal of the Chinese Society of Rare Earths, 2010, 28(6): 709-715.
朱福良, 黄秀扬, 余细波, 等. 热处理温度对铕掺杂Ti /SnO_2-Sb电极性能的影响[J]. 中国稀土学报, 2010, 28(6): 709-715.
15 Kresse G, Furthmuller J. Efficiency of ab-initio total energy calculations for metals and semiconductors using a plane-wave basis set[J]. Comput Mater Sci 1996, 6(1): 15-50.
16 Marlo M, Milman V. Density-functional study of bulk and surface properties of titanium nitride using different exchange correlation functional[J]. Phys Rev B, 2000, 62(4): 2899.
17 Zhang Fuchun, Zhang Zhiyong, Zhang Weihu, *et al*.. The first-principle calculation of electronic structure and optical properties of In_2O_3[J]. Acta Chimica Sinica, 2008, 66(16): 1863-1868.
张富春, 张志勇, 张威虎, 等. In_2O_3电子结构与光学性质的第一性原理计算[J]. 化学学报, 2008, 66(16): 1863-1868.
18 Milman V, Winkler B, White J A, *et al*.. Electronic structure, properties, and phase stabilities of inorganic crystals: A pseudo potential plane-wavestudy[J]. Quantum Chem, 2000, 77(5): 895-910.
19 Thangaraju B. Structural and electrical studies on highly conducting spray deposited fluorine and antimony doped SnO_2 thin films from $SnCl_2$ precursor[J]. Thin Solid Films, 2002, 402(1): 71-78.
20 Zhang Fuchun, Deng Zhouhu, Yang Junfeng, *et al*.. First- principles calculation of electronic structure and optical properties of ZnO[J]. Acta Optica Sinica 2006, 26(8): 1203-1209.
张富春, 邓周虎, 阎军锋, 等. ZnO电子结构与光学性质的第一性原理计算[J]. 光学学报, 2006, 26(8): 1203-1209.
21 Borges P D, Scolfaro L M R, Alves H W L, *et al*.. DFT study of the electronic, vibrational, and optical properties of SnO_2 [J]. Chem Acc, 2010, 126(1): 39-44.
22 Duan M Y, Xu M, Zhou H P, *et al*.. Electronic structure and optical properties of ZnO doped with carbon[J]. Acta Phys Sin, 2008, 57(10): 6520-6525.
段满益, 徐 明, 周海平, 等. 碳掺杂ZnO的电子结构和光学性质[J]. 物理学报, 2008, 57(10): 6520-6525.
23 Guo Yuzhong, Wang Jianhua, Huang Ruian, *et al*.. Electrical and optical properties of transparent and conductive Sb-doped SnO_2 films[J]. Journal of Inorganic Materials, 2002, 17(1): 131-138.
郭玉忠, 王剑华, 黄瑞安, 等. 掺杂SnO_2透明导电薄膜电学及光学性能研究[J]. 无机材料学报, 2002, 17(1): 131-138.
24 Rahman G, Victor M, Garcia S. Surface- induced magnetism in C-doped SnO_2[J]. Appl Phys Lett, 2010, 96(5): 052508.

栏目编辑：张浩佳